Version of 22 April 2025

A filtered finite difference method for a highly oscillatory nonlinear Klein–Gordon equation

Yanyan Shi[1], **Christian Lubich**[1]

arXiv:2504.19359v1 [math.NA] 27 Apr 2025

Abstract We consider a nonlinear Klein–Gordon equation in the nonrelativistic limit regime with highly oscillatory initial data in the form of a modulated plane wave. In this regime, the solution exhibits rapid oscillations in both time and space, posing challenges for numerical approximation. We propose a filtered finite difference method that achieves second-order accuracy with time steps and mesh sizes that are not restricted in magnitude by the small parameter. Moreover, the method is uniformly convergent in the range from arbitrarily small to moderately bounded scaling parameters. Numerical experiments illustrate the theoretical results.

Keywords. finite difference method, filter, nonlinear Klein–Gordon equation, highly oscillatory, asymptotic-preserving, uniformly accurate

Mathematics Subject Classification (2020): 65M06, 65M12, 65M15

1 Introduction

We consider the numerical solution of nonlinear dispersive wave equations, which often exhibit highly oscillatory behavior in both time and space. As a concrete example, we focus on the nonlinear Klein–Gordon equation in the same scaling as, e.g., in [2,1,9,5]: with a small parameter $0 < \varepsilon \leqslant 1$, we consider

$$\varepsilon^2 \partial_{tt} u - \partial_{xx} u + \frac{1}{\varepsilon^2} u + \lambda |u|^2 u = 0, \qquad x \in \mathbb{R},\ 0 \leqslant t \leqslant T, \tag{1.1}$$

where the solution $u = u(t,x)$ is complex-valued. Here, T is a fixed final time independent of ε, and λ is a fixed nonzero real number. The initial conditions

[1] Mathematisches Institut, Univ. Tübingen, D-72076 Tübingen, Germany.
E-mail: {Shi, Lubich}@na.uni-tuebingen.de

are given by modulated plane waves,

$$u(0,x) = a_0(x)e^{\mathrm{i}\kappa x/\varepsilon}, \quad \partial_t u(0,x) = \frac{1}{\varepsilon^2} b_0(x)e^{\mathrm{i}\kappa x/\varepsilon}. \tag{1.2}$$

The initial conditions include a rapidly oscillating phase factor with a fixed wave vector $\kappa \in \mathbb{R}\backslash\{0\}$, characterizing the dominant wavenumber of the initial wave packet. The functions $a_0, b_0 : \mathbb{R} \to \mathbb{C}$ are smooth profiles whose derivatives are uniformly bounded independently of ε and which have bounded support. Our objective is to study the solution in the nonrelativistic limit regime, i.e. $0 < \varepsilon \ll 1$, over a fixed time interval $0 \leqslant t \leqslant T$.

Numerically solving (1.1) is challenging due to the high oscillations of the solution in both time and space. The literature predominantly focuses on handling temporal oscillations, with methods including finite difference schemes [2], Gautschi-type exponential integrators [10], time-splitting techniques [8], two-scale methods [6,3], approaches based on Duhamel's formula [5], and on multiscale expansions [9,1]. However, relatively few works address spatial and time oscillations at the same time for (1.1) or similar equations, with exceptions including the nonlinear geometric optics method [7] and analytical approximations [11].

In this work, we build on the approach in [15], adapting it to a different equation. By introducing suitable filter functions into the standard finite difference scheme, we enable the use of large time steps and mesh sizes that are not constrained by the small parameter ε. Our method employs co-moving coordinates, which allows us to maintain a relatively small spatial computational interval that is largely determined by the support of the initial conditions, while capturing the original solution across the entire domain. Furthermore, our approach can effectively resolve counterpropagating waves, as the solution exhibits two opposite time frequencies corresponding to distinct group velocities. The proposed method is not only asymptotic preserving as $\varepsilon \to 0$ but also uniformly accurate, recovering a standard co-moving leapfrog scheme when the ratio of the time step and mesh size to ε approaches zero.

Section 2 presents an approximate solution to the continuous problem for small ε. In Section 3, we introduce the filtered finite difference method and state the main results of this paper. We derive the dominant term in the modulated Fourier expansion of the numerical solution and establish second-order error bounds, allowing step sizes τ and mesh widths h that can be arbitrarily large compared to ε. For $h \gg \varepsilon$, the method imposes a stepsize restriction, $\tau \leqslant ch^2$, but the step size τ and mesh width h remain linked by a consistency condition.

The results of Section 3 are proved in Sections 4 and 5. In Section 4, we analyze the consistency error, i.e., the defect arising when inserting a function with a controlled small distance to the exact solution into the numerical scheme. Section 5 presents a linear Fourier stability analysis, followed by a nonlinear stability analysis that bounds the numerical solution error in terms of the defect. Finally, Section 6 provides numerical experiments illustrating our theoretical findings.

2 Dominant term of the exact solution

Before introducing the numerical method, we establish the following approximation of the exact solution. Note that the velocity behaves as $\partial_t u = O(\varepsilon^{-2})$ so that the error bound given below corresponds to the relative error.

Proposition 2.1 *There exists a positive constant c such that*

$$\begin{aligned} \|u(t,\cdot) - u_{app}(t,\cdot)\|_{L^\infty} &\leqslant c\,\varepsilon, \quad 0 \leqslant t \leqslant T, \\ \varepsilon^2 \|\partial_t u(t,\cdot) - \partial_t u_{app}(t,\cdot)\|_{L^\infty} &\leqslant c\,\varepsilon, \quad 0 \leqslant t \leqslant T \end{aligned}$$

where u_{app} has the form

$$u_{app}(t,x) = a^+(t,\xi^+)e^{\mathrm{i}(\kappa x - \omega t/\varepsilon)/\varepsilon} + a^-(t,\xi^-)e^{\mathrm{i}(\kappa x + \omega t/\varepsilon)/\varepsilon}, \tag{2.1}$$

with $\xi^\pm = x \mp c_g t/\varepsilon$, frequency $\omega = \sqrt{1+\kappa^2}$, and the group velocity $c_g = \partial_\kappa \omega = \kappa/\omega < 1$. The functions $a^+(t,\xi^+)$ and $a^-(t,\xi^-)$ satisfy the following nonlinear Schrödinger equations:

$$\begin{aligned} 2\mathrm{i}\omega\partial_t a^+ &= -(1-c_g^2)\,\partial^2_{\xi^+} a^+ + \lambda|a^+|^2 a^+, \quad a^+(0,\xi^+) = \frac{a_0(\xi^+) + \mathrm{i}b_0(\xi^+)/\omega}{2}, \\ -2\mathrm{i}\omega\partial_t a^- &= -(1-c_g^2)\,\partial^2_{\xi^-} a^- + \lambda|a^-|^2 a^-, \quad a^-(0,\xi^-) = \frac{a_0(\xi^-) - \mathrm{i}b_0(\xi^-)/\omega}{2}. \end{aligned} \tag{2.2}$$

Proof Rather than directly estimating the error between u and u_{app}, we introduce a higher-order approximation as in [14]:

$$\begin{aligned} U_{\mathrm{app}}(t,x) = {} & \left(a^+ + \varepsilon b^+\right) e^{\mathrm{i}(\kappa x - \omega t/\varepsilon)/\varepsilon} + \left(a^- + \varepsilon b^-\right) e^{\mathrm{i}(\kappa x + \omega t/\varepsilon)/\varepsilon} \\ & - \frac{\varepsilon^2 \lambda}{\kappa^2 - 9\omega^2 + 1}\left((a^+)^2\overline{a^-}e^{\mathrm{i}(\kappa x - 3\omega t/\varepsilon)/\varepsilon} + \overline{a^+}(a^-)^2 e^{\mathrm{i}(\kappa x + 3\omega t/\varepsilon)/\varepsilon}\right), \end{aligned}$$

where $a^+ = a^+(t,\xi^+)$, $a^- = a^-(t,\xi^-)$ satisfy (2.2), and $b^+ = b^+(t,\xi^+,\xi^-)$, $b^- = b^-(t,\xi^+,\xi^-)$ satisfy the following equations

$$4\mathrm{i}\kappa\partial_{\xi^-} b^+ = 2\lambda|a^-|^2 a^+, \quad 4\mathrm{i}\kappa\partial_{\xi^+} b^- = 2\lambda|a^+|^2 a^-. \tag{2.3}$$

The defect obtained on inserting U_{app} into (1.1) is

$$d(t,x) = \varepsilon^2 \partial_{tt} U_{\mathrm{app}} - \Delta_x U_{\mathrm{app}} + \frac{1}{\varepsilon^2} U_{\mathrm{app}} + \lambda|U_{\mathrm{app}}|^2 U_{\mathrm{app}}. \tag{2.4}$$

Using the expression of $U_{\rm app}$, we have

$$\begin{aligned} d(t,x) =& \Big(-2\mathrm{i}\omega\partial_t a^+ + (c_g^2-1)\partial_{\xi^+}^2 a^+ - 4\mathrm{i}\kappa\partial_{\xi^-} b^+ \\ &\qquad +\lambda(|a^+|^2 a^+ + 2|a^-|^2 a^+)\Big) e^{\mathrm{i}(\kappa x-\omega t/\varepsilon)/\varepsilon} \\ &+\Big(2\mathrm{i}\omega\partial_t a^- + (c_g^2-1)\partial_{\xi^-}^2 a^- - 4\mathrm{i}\kappa\partial_{\xi^+} b^- \\ &\qquad +\lambda(|a^-|^2 a^- + 2|a^+|^2 a^-)\Big) e^{\mathrm{i}(\kappa x+\omega t/\varepsilon)/\varepsilon} \\ &+\left(\frac{(9\omega^2-\kappa^2-1)\lambda}{\kappa^2-9\omega^2+1}+\lambda\right)(a^+)^2\overline{a^-}e^{\mathrm{i}(\kappa x-3\omega t/\varepsilon)/\varepsilon} \\ &+\left(\frac{(9\omega^2-\kappa^2-1)\lambda}{\kappa^2-9\omega^2+1}+\lambda\right)(a^-)^2\overline{a^+}e^{\mathrm{i}(\kappa x+3\omega t/\varepsilon)/\varepsilon} + O(\varepsilon). \end{aligned}$$

Since $a^\pm$ and $b^\pm$ satisfy the equations (2.2) and (2.3), we have

$$\|d(t,x)\| = O(\varepsilon),$$

where the norm can be either the maximum norm or the Wiener norm introduced in Section 4.2. Comparing equation (2.4) with (1.1) shows that the error $e = u - U_{\rm app}$ solves the evolution equation

$$\varepsilon^2\partial_{tt}e - \Delta_x e + \frac{1}{\varepsilon^2}e + \lambda(|u|^2u - |U_{\rm app}|^2U_{\rm app}) + d = 0.$$

Rewriting this equation as a first-order system results

$$\partial_t\begin{pmatrix}e\\ s\\ p\end{pmatrix} = \frac{1}{\varepsilon}\begin{pmatrix}0&0&0\\0&0&\partial_x\\0&\partial_x&0\end{pmatrix}\begin{pmatrix}e\\ s\\ p\end{pmatrix} - \frac{1}{\varepsilon^2}\begin{pmatrix}0&-1&0\\1&0&0\\0&0&0\end{pmatrix}\begin{pmatrix}e\\ s\\ p\end{pmatrix} - \begin{pmatrix}0\\ \lambda(|u|^2u-|U_{\rm app}|^2U_{\rm app})+d\\ 0\end{pmatrix},$$

with $s = \varepsilon^2\partial_t e$ and $p = \varepsilon\partial_x u$. Applying the technique from [4, Lemma 5.2] then leads to the desired result. □

Remark 2.1 Similar results can be found in [13,14], where a different scaling is considered. Notably, using the Wiener norm yields a sharper estimate, improving the order of accuracy by 1/2 compared to the results in [14].

3 Numerical method and main results

Our numerical method is designed for the co-moving coordinate

$$\xi = x - \mu t/\varepsilon, \quad w(t,\xi) = w(t, x-\mu t/\varepsilon) = u(t,x),$$

where μ is a constant to be chosen. The change of variables transforms the original problem (1.1) into the following form

$$\varepsilon^2\partial_{tt}w - 2\varepsilon\mu\partial_t\partial_\xi w + (\mu^2-1)\Delta_\xi w + \frac{1}{\varepsilon^2}w + \lambda|w|^2w = 0, \tag{3.1}$$

which is defined on the time interval $[0, T]$.

For simplicity of presentation, we introduce our filtered finite difference method in the context of one spatial dimension, $0 \leqslant \xi \leqslant 2\pi$, with periodic boundary conditions. Let the time step be $\tau = T/N > 0$ and the mesh size $h = 2\pi/M > 0$, where N and M are positive integers. We denote by w_j^n the numerical approximation of $w(t_n, \xi_j)$, where $t_n = n\tau$ for $0 \leqslant n \leqslant N$, and $\xi_j = jh$ for $0 \leqslant j \leqslant M$. The numerical methods and the theoretical results for them can be extended to higher spatial dimensions without additional difficulty.

Filtered finite difference algorithm. We now introduce an explicit algorithm for solving (3.1), which has the symmetric two-step formulation:

$$\begin{aligned} \varepsilon^2 \frac{w_j^{n+1} - 2\phi_1(\alpha) w_j^n + w_j^{n-1}}{\tau^2 \psi_1(\alpha)} - 2\varepsilon\mu \frac{(w_{j+1}^{n+1} - w_{j+1}^{n-1}) - (w_{j-1}^{n+1} - w_{j-1}^{n-1})}{4\mathrm{sinc}(\alpha)\mathrm{sinc}(\beta)\tau h} \\ + (\mu^2 - 1) \frac{w_{j+1}^n - 2\phi_2(\beta) w_j^n + w_{j-1}^n}{h^2 \psi_2(\beta)} + \frac{1}{\varepsilon^2} w_j^n + \lambda \frac{|w_j^n|^2 w_j^n}{\mathrm{tanc}^2(\beta)} = 0 \end{aligned} \tag{3.2}$$

with $\mathrm{sinc}(z) = \sin(z)/z$ and $\mathrm{tanc}(z) = \tan(z)/z$, where

$$\begin{aligned} \phi_1(z) &= \frac{3}{2}\mathrm{sinc}(z) - \frac{1}{2}\cos(z), \quad \psi_1(z) = \frac{\phi_1(z) - \cos(z)}{z^2/2}, \\ \phi_2(z) &= \cos(z) + \frac{1}{2}\sin(z)\tan(z), \quad \psi_2(z) = \frac{\phi_2(z) - \cos(z)}{z^2/2}, \\ \alpha &= (\kappa c_g - \omega)\tau/\varepsilon^2, \quad \beta = \kappa h/\varepsilon. \end{aligned}$$

The velocity is approximated as

$$v_j^n = \frac{-\omega}{\kappa\mu - \omega} \frac{w_j^{n+1} - w_j^{n-1}}{2\tau\mathrm{sinc}(\alpha)}. \tag{3.3}$$

The extra factor $-\omega/(\kappa\mu - \omega)$ accounts for the transformation between u and w.

Note that as $z \to 0$, we have $\mathrm{sinc}(z) = 1 + O(z^2)$, $\mathrm{tanc}(z) = 1 + O(z^2)$, and $\phi_i(z) = 1 + O(z^4)$, $\psi_i(z) = 1 + O(z^2)$ for $i = 1, 2$. Therefore, the filtered finite difference algorithm tends to the classical leapfrog scheme in the limit $\tau/\varepsilon \to 0$ and $h/\varepsilon \to 0$. Our primary interest here, however, is in using the filtered scheme for large ratios τ/ε and h/ε.

To solve the original equation (1.1) with $h \gg \varepsilon$ and $\tau \gg \varepsilon^2$, we apply the numerical scheme (3.2) twice, each time with a different μ corresponding to one of the two opposite group velocities. The final solution is then obtained by combining the results. The procedure is detailed below.

Algorithm 3.1 *Denote the time step by $\tau = T/N$ and the mesh size by $h = 2\pi/M$.*

1. *Solve* (3.2) *on* $[0, 2\pi]$ *with* $\mu = c_g$ *and initial data*

$$w^+(0,\xi) = a^+(0,\xi)e^{\mathrm{i}\kappa\xi/\varepsilon}, \quad \partial_t w^+(0,\xi) = -\frac{\mathrm{i}\omega}{\varepsilon^2}a^+(0,\xi)e^{\mathrm{i}\kappa\xi/\varepsilon}.$$

   This yields the numerical solution $w_j^{+,n}$ *for* $j = 0, \dots, M$*. The numerical velocity* $v_j^{+,n}$ *is obtained by* (3.3)*.*
2. *Solve* (3.2) *again on* $[0, 2\pi]$ *with* $\mu = -c_g$ *(i.e., reversing the signs* $\omega \to -\omega$ *and* $c_g \to -c_g$*), using initial data*

$$w^-(0,\xi) = a^-(0,\xi)e^{\mathrm{i}\kappa\xi/\varepsilon}, \quad \partial_t w^-(0,\xi) = \frac{\mathrm{i}\omega}{\varepsilon^2}a^-(0,\xi)e^{\mathrm{i}\kappa\xi/\varepsilon}.$$

   This yields the numerical solution $w_j^{-,n}$ *for* $j = 0, \dots, M$*. The numerical velocity* $v_j^{-,n}$ *is obtained by* (3.3)*.*
3. *Assume* $t_n \geqslant \varepsilon\pi/c_g$*, meaning the wave packets remain well separated, the final approximation to the original equation is obtained by combining the two solutions:*

$$u^n(\xi_j + c_g t_n/\varepsilon) = w_j^{+,n}, \quad u^n(\xi_j - c_g t_n/\varepsilon) = w_j^{-,n},$$
$$v^n(\xi_j + c_g t_n/\varepsilon) = v_j^{+,n}, \quad v^n(\xi_j - c_g t_n/\varepsilon) = v_j^{-,n}.$$

Remark 3.1 If the wave packets overlap, the solution is obtained through interpolation:

$$u_j^n = \mathcal{I}(\{w_j^{+,n}\}, x_j) + \mathcal{I}(\{w_j^{-,n}\}, x_j),$$
$$v_j^n = \mathcal{I}(\{v_j^{+,n}\}, x_j) + \mathcal{I}(\{v_j^{-,n}\}, x_j),$$

where $\mathcal{I}$ denotes an interpolation operator ensuring a smooth transition between $\{w_j^{+,n}\}$ and $\{w_j^{-,n}\}$ in the overlapping region. For long-time simulations or small ε, the separation condition $t_n \geqslant \varepsilon\pi/c_g$ is typically satisfied, making interpolation unnecessary.

Remark 3.2 For large ε including $\varepsilon = 1$, the original equation (1.1) is equivalent to (3.1) with $\mu = 0$. In this case, we set $\mu = 0$ in both the second and third terms of the scheme (3.2), as well as in the factor of (3.3). The method is then applied once using the initial data (1.2), which reduces the scheme to the filtered leapfrog method for the original equation (1.1).

The following result (Theorem 3.1) provides the dominant term of the modulated Fourier expansion of the numerical solution to (3.2). To ensure that the numerical method captures the same dominant term, we require a relation between ε, τ, and h. The step size and mesh width are chosen such that $\alpha = (\kappa c_g - \omega)\tau/\varepsilon^2$, $\beta = \kappa h/\varepsilon$ satisfy the following *consistency condition*: For a fixed nonzero real number ρ,

$$-\frac{\varepsilon^4 \sin(\alpha)}{\omega\tau\psi_1(\alpha)} = \frac{\varepsilon^2}{\operatorname{tanc}^2(\beta)} = \rho. \tag{3.4}$$

This ensures that the profile functions $a^{\pm}$ satisfy the same equation (2.2) as in the exact solution.

We also impose the following *stability condition*: for a fixed $r < 1$,

$$|\phi_1(\alpha)| + \frac{\tau^2|c_g^2 - 1|}{\varepsilon^2 h^2}\frac{1 + |\phi_2(\beta)|}{|\psi_2(\beta)|}|\psi_1(\alpha)| + \frac{\tau^2}{2\varepsilon^4}|\psi_1(\alpha)| \leqslant r < 1. \tag{3.5}$$

When $h \gg \varepsilon$ and $\cos(\beta)$ is bounded away from 0, the second term on the left-hand side is proportional to τ/h^2, since

$$\psi_1(\alpha) = -\frac{\varepsilon^4 \sin(\alpha)}{\omega\tau\rho}, \quad \frac{1}{\psi_2(\beta)} = \frac{\rho}{\varepsilon^2\cos(\beta)}$$

by (3.4). Hence, condition (3.5) simplifies to requiring that τ/h^2 remains bounded by a sufficiently small constant, independent of ε.

Theorem 3.1 (Dominant term of the numerical solution) *Let $w_j^{+,n}$ be the numerical solution obtained using the filtered finite difference algorithm* (3.2)*, under the stability condition* (3.5) *and the consistency condition* (3.4)*. Assume that the solution $a^+(t,\xi)$ of the nonlinear Schrödinger equation* (2.2) *has sufficiently many bounded partial derivatives (we assume $a \in C^4([0,T] \times \mathbb{T})$). Then the numerical solution $w_j^{+,n}$ can be written as*

$$w_j^{+,n} = a^+(t,\xi)\,\mathrm{e}^{\mathrm{i}\kappa\xi/\varepsilon}\mathrm{e}^{\mathrm{i}(\kappa c_g - \omega)t/\varepsilon^2} + R^+(t,\xi),$$

for $t = n\tau \leqslant T$ and $\xi = jh$, where $a^+(t,\xi)$ satisfies the first equation in (2.2)*, and the remainder term is bounded by*

$$\|R^+\|_{C([0,T]\times\mathbb{T})} \leqslant C(\tau^2 + h^2 + \varepsilon^2).$$

Here, C is independent of ε, τ, h, but depends on ρ, r, and the final time T.

Remark 3.3 For $w_j^{-,n}$ obtained in the second step of Algorithm 3.1, we have an analogous result:

$$w_j^{-,n} = a^-(t,\xi)\,\mathrm{e}^{\mathrm{i}\kappa\xi/\varepsilon}\mathrm{e}^{-\mathrm{i}(\kappa c_g - \omega)t/\varepsilon^2} + R^-(t,\xi),$$

where $a^-(t,\xi)$ satisfies the second equation in (2.2) and R^- has the same bound as given for R^+. The proof follows the same steps as Theorem 3.1 and is therefore omitted.

A further main result of this paper is the following error bound for the filtered finite difference method. It follows directly from Algorithm 3.1, the numerical and exact solution representations in Theorem 3.1, and Lemma 2.1. Note that the velocity behaves as $\partial_t u = O(\varepsilon^{-2})$ so that the error bound given below corresponds to the relative error.

Theorem 3.2 (Error bound) *Under the assumptions of Theorem 3.1 and assuming that the wave packets remain well separated, we obtain the error estimates*

$$|u(t_n, \xi_j \pm c_g t_n/\varepsilon) - u^n(\xi_j \pm c_g t_n/\varepsilon)| = O(\tau^2 + h^2 + \varepsilon),$$
$$\varepsilon^2 |\partial_t u(t_n, \xi_j \pm c_g t_n/\varepsilon) - v^n(\xi_j \pm c_g t_n/\varepsilon)| = O(\tau^2 + h^2 + \varepsilon),$$

uniformly for $t_n = n\tau \leqslant T$ and $\xi_j = jh$. The constant symbolized by the O-notation is independent of ε, the time step τ, and the mesh size h, provided that the consistency condition (3.4) *and the stability condition* (3.5) *hold. It is also independent of j and n with $n\tau \leqslant T$.*

Remark 3.4 In the less interesting regime where $\tau \ll \varepsilon^2$ and $h \ll \varepsilon$, a standard Taylor series error analysis yields an error bound of $O(\tau^2/\varepsilon^6 + h^2/\varepsilon^4)$. Consequently, the error satisfies

$$|u(t_n, \xi_j \pm c_g t/\varepsilon) - u^n(\xi_j \pm c_g t/\varepsilon)| \leqslant \min\left(C_0(\tau^2 + h^2 + \varepsilon), C_1\left(\frac{\tau^2}{\varepsilon^6} + \frac{h^2}{\varepsilon^4}\right)\right)$$

uniformly for $t_n = n\tau \leqslant T$, $\xi_j = jh$, and $0 < \varepsilon \leqslant 1$. Maximizing this bound over $0 < \varepsilon \leqslant 1$ gives the optimal balance $\varepsilon^7 \sim \tau^2, \varepsilon^5 \sim h^2$, leading to a uniform accuracy of $O\big(\tau^{2/7} + h^{4/7}\big)$ in the maximum norm for all $0 < \varepsilon \leqslant 1$. The optimal quadratic convergence rate is achieved when $\varepsilon \sim 1$ or $\varepsilon \leqslant \tau^2 + h^2$.

4 Consistency

With the solution $a^+(t, \xi)$ of the first nonlinear Schrödinger initial value problem in (2.2), we denote

$$A^+(t, \xi) = a^+(t, \xi)\, \mathrm{e}^{\mathrm{i}\kappa\xi/\varepsilon} \mathrm{e}^{\mathrm{i}(\kappa c_g - \omega)t/\varepsilon^2}. \tag{4.1}$$

Using the notations

$$\exp(\tau\partial_t)u(t, \xi) = u(t + \tau, \xi), \quad \exp(h\partial_\xi)u(t, \xi) = u(t, \xi + h),$$

we consider the defect obtained on inserting $A^+(\tau, \xi)$ into the filtered finite difference scheme (3.2),

$$\begin{aligned} d(t, \xi) :=& \varepsilon^4 \frac{\exp(\tau\partial_t) - 2\phi_1(\alpha) + \exp(-\tau\partial_t)}{\tau^2\, \psi_1(\alpha)} A^+(t, \xi) \\ &- 2\varepsilon^3 c_g \frac{(\exp(\tau\partial_t) - \exp(-\tau\partial_t))(\exp(h\partial_\xi) - \exp(-h\partial_\xi))}{4\mathrm{sinc}(\alpha)\mathrm{sinc}(\beta)\tau h} A^+(t, \xi) \\ &+ \varepsilon^2 (c_g^2 - 1) \frac{\exp(h\partial_\xi) - 2\phi_2(\beta) + \exp(-h\partial_\xi)}{h^2\, \psi_2(\beta)} A^+(t, \xi) \\ &+ \lambda\varepsilon^2 \frac{|A^+(t, x)|^2 A^+(t, \xi)}{\mathrm{tanc}^2(\beta)} \end{aligned} \tag{4.2}$$

4.1 Defect bound in the maximum norm

Lemma 4.1 *In the situation of Theorem 3.1, the defect* (4.2) *is bounded in the maximum norm by*

$$\|d\|_{C([0,T]\times\mathbb{T})} \leqslant c(\tau^2 + h^2 + \varepsilon^2),$$

where c is independent of ε, τ, h and n with $t_n = n\tau \leqslant T$.

Proof We note

$$\begin{aligned}
&(\exp(\tau\partial_t) - \exp(-\tau\partial_t))A^+(t,\xi) \\
&= 2\Big(\mathrm{i}\,\sin(\alpha)\,a^+ + \tau\,\cos(\alpha)\,\partial_t a^+ + \frac{\mathrm{i}\tau^2}{2}\,\sin(\alpha)\,\partial_t^2 a^+ + O(\tau^3)\Big)\,\mathrm{e}^{\mathrm{i}\kappa\xi/\varepsilon}\mathrm{e}^{(\kappa c_g-\omega)t/\varepsilon^2},
\end{aligned} \tag{4.3}$$

and

$$\begin{aligned}
&(\exp(\tau\partial_t) + \exp(-\tau\partial_t))A^+(t,\xi) \\
&= 2\Big(\cos(\alpha)\,a^+ + \mathrm{i}\tau\,\sin(\alpha)\,\partial_t a^+ + \frac{\tau^2}{2}\cos(\alpha)\,\partial_t^2 a^+ + O(\tau^3)\Big)\,\mathrm{e}^{\mathrm{i}\kappa\xi/\varepsilon}\mathrm{e}^{(\kappa c_g-\omega)t/\varepsilon^2},
\end{aligned}$$

where a^+ and its partial derivatives are evaluated at (t,ξ). Similar expressions can be derived for the spatial discretization.

Then we have

$$\begin{aligned}
&\varepsilon^4\,\frac{\exp(\tau\partial_t) - 2\phi_1(\alpha) + \exp(-\tau\partial_t)}{\tau^2\,\psi_1(\alpha)}A^+(t,\xi) \\
&= \Big(\frac{-\varepsilon^4\alpha^2}{\tau^2}\,a^+ + \frac{2\mathrm{i}\varepsilon^4}{\tau\psi_1(\alpha)}\,\sin(\alpha)\,\partial_t a^+ + O(\tau^2+\varepsilon^2)\Big)\,\mathrm{e}^{\mathrm{i}\kappa\xi/\varepsilon}\mathrm{e}^{(\kappa c_g-\omega)t/\varepsilon^2}.
\end{aligned}$$

Here, the $O(\tau^2+\varepsilon^2)$ term requires an explanation: The factor multiplying $\partial_t^2 a^+$ equals

$$\begin{aligned}
\frac{\varepsilon^4\cos(\alpha)}{\psi_1(\alpha)} &= \varepsilon^4\left(\frac{\cos(\alpha)-\operatorname{sinc}(\alpha)}{\psi_1(\alpha)} + \frac{\operatorname{sinc}(\alpha)}{\psi_1(\alpha)}\right) \\
&= -\tfrac{1}{3}\varepsilon^4\alpha^2 - \varepsilon^2\frac{\rho\omega}{\kappa c_g-\omega} \\
&= -\tfrac{1}{3}(\kappa c_g-\omega)^2\tau^2 - \varepsilon^2\frac{\rho\omega}{\kappa c_g-\omega},
\end{aligned}$$

where we used the first equation of (3.4) in the second equality. This argument yields the $O(\tau^2+\varepsilon^2)$ term above.

Similarly, we have

$$\begin{aligned}
&\varepsilon^2(c_g^2-1)\,\frac{\exp(h\partial_\xi) - 2\phi_2(\beta) + \exp(-h\partial_\xi)}{h^2\,\psi_2(\beta)}A^+(t,\xi) \\
&= \frac{\varepsilon^2(c_g^2-1)}{\psi_2(\beta)}\Big(\frac{-\beta^2\psi_2(\beta)}{h^2}\,a^+ + \frac{2\mathrm{i}}{h}\,\sin(\beta)\,\partial_\xi a^+ + \cos(\beta)\partial_\xi^2 a^+ + O(h^2)\Big)\,\mathrm{e}^{\mathrm{i}\kappa\xi/\varepsilon}\mathrm{e}^{(\kappa c_g-\omega)t/\varepsilon^2}.
\end{aligned}$$

For the second term appearing in the defect $d(t,\xi)$, we have

$$\begin{aligned}
&2\varepsilon^3 c_g \, \frac{(\exp(\tau\partial_t)-\exp(-\tau\partial_t))(\exp(h\partial_\xi)-\exp(-h\partial_\xi))}{4\mathrm{sinc}(\alpha)\mathrm{sinc}(\beta)\tau h} A^+(t,\xi) \\
&= 2\varepsilon^3 c_g \left(\frac{\mathrm{i}\kappa}{\varepsilon}(1+h^2\partial_\xi^2+\cdots) + \frac{1}{\mathrm{tanc}(\beta)}(\partial_\xi + h^2\partial_\xi^3+\cdots) \right) \\
&\quad \left(\frac{\mathrm{i}(\kappa c_g-\omega)}{\varepsilon^2}(1+\tau^2\partial_t^2+\cdots) + \frac{1}{\mathrm{tanc}(\alpha)}(\partial_t+\tau^2\partial_t^3+\cdots) \right) a^+ \\
&= -2c_g\kappa(\kappa c_g-\omega)a^+ + 2\varepsilon c_g \frac{\mathrm{i}(\kappa c_g-\omega)}{\mathrm{tanc}(\beta)}\partial_\xi a^+ + O(h^2+\tau^2+\varepsilon^2).
\end{aligned}$$

Here, the $O(h^2+\tau^2+\varepsilon^2)$ term uses the observation that $1/\mathrm{tanc}(\beta) = \sqrt{\rho}/\varepsilon$ and

$$\begin{aligned}
\frac{1}{\mathrm{tanc}(\alpha)} &= \frac{\cos(\alpha)-\mathrm{sinc}(\alpha)}{\mathrm{sinc}(\alpha)} + 1 \\
&= -\frac{\alpha^2\psi_1(\alpha)}{3\mathrm{sinc}(\alpha)} + 1 \\
&= \frac{\tau^2}{\varepsilon^2}\frac{\kappa c_g-\omega}{3\rho\omega} + \frac{\varepsilon^2}{\varepsilon^2}
\end{aligned}$$

where we used the first equation of (3.4) in the last equality.

Finally we obtain

$$\begin{aligned}
d(t,\xi) = &\underbrace{\left(-\varepsilon^4\alpha^2/\tau^2 - \varepsilon^2(c_g^2-1)\beta^2/h^2 + 2c_g\kappa(\kappa c_g-\omega)+1\right)}_{=0} a^+ \\
&+ \underbrace{\left(\frac{2\mathrm{i}\varepsilon^2(c_g^2-1)}{h\psi_2(\beta)}\,\sin(\beta) - 2\varepsilon c_g \frac{\mathrm{i}(\kappa c_g-\omega)}{\mathrm{tanc}(\beta)} \right)}_{=0} \partial_\xi a^+ \qquad (4.4) \\
&+ \frac{\varepsilon^2}{\mathrm{tanc}^2(\beta)} \underbrace{\left(-2\mathrm{i}\omega\partial_t a^+ + (c_g^2-1)\,\partial_\xi^2 a^+ + \lambda\,|a^+|^2 a^+ \right)}_{=0} \qquad (4.5) \\
&+ O(\tau^2+h^2+\varepsilon^2) \qquad (4.6)
\end{aligned}$$

by (3.4). This yields the stated result. □

However, the maximum norm in the defect bound of Lemma 4.1 turns out to be too weak a norm for the proof of Theorems 3.1 and 3.2.

4.2 Defect bound in the Wiener algebra norm

Let $A(\mathbb{T})$ be the space of 2π-periodic complex-valued functions with absolutely convergent Fourier series $f(x) = \sum_{k=-\infty}^{\infty} \widehat{f}(n)\,\mathrm{e}^{\mathrm{i}kx}$, equipped with the $\ell^1(\mathbb{Z})$

norm of the sequence of Fourier coefficients. For the pointwise product of two functions $f, g \in A(\mathbb{T})$ we then have (see, e.g., [12, Section I.6])

$$\|fg\|_{A(\mathbb{T})} \leqslant \|f\|_{A(\mathbb{T})} \, \|g\|_{A(\mathbb{T})}, \tag{4.7}$$

which makes $A(\mathbb{T})$ a Banach algebra, known as the Wiener algebra. Note that the maximum norm of a function in $A(\mathbb{T})$ is bounded by its $A(\mathbb{T})$-norm, and conversely, the $A(\mathbb{T})$-norm is bounded by the maximum norm of the function and its derivative, see [12, Section I.6]:

$$\|f\|_{C(\mathbb{T})} \leqslant \|f\|_{A(\mathbb{T})} \quad \text{and} \quad \|f\|_{A(\mathbb{T})} \leqslant c_1 \, \|f\|_{C^1(\mathbb{T})}. \tag{4.8}$$

The space $C([0,T], A(\mathbb{T}))$ is the Banach space of $A(\mathbb{T})$-valued continuous functions on the interval $[0,T]$, with $\|d\|_{C([0,T],A(\mathbb{T}))} = \max_{0\leqslant t\leqslant T} \|d(t,\cdot)\|_{A(\mathbb{T})}$.

Lemma 4.2 *In the situation of Theorem 3.1, the defect* (4.2) *is bounded in the Wiener algebra norm by*

$$\|d\|_{C([0,T],A(\mathbb{T}))} \leqslant c(\tau^2 + h^2 + \varepsilon^2),$$

where c is independent of ε, τ, h, and n with $t_n = n\tau \leqslant T$.

Proof The proof follows the same steps as the proof in [15, Lemma 3.2].

5 Stability

5.1 Linear stability analysis in the Wiener algebra

In this subsection we give linear stability results for the filtered finite difference scheme. We bound numerical solution corresponding to the linear Klein–Gordon equation (1.1) (without the nonlinearity) in the Wiener algebra norm, using Fourier analysis.

We momentarily omit the nonlinearity and interpolate the filtered finite difference scheme (3.2) (with $\mu = c_g$) from discrete spatial points $\xi_j = jh$ to arbitrary $\xi \in \mathbb{T}$ by setting

$$\begin{aligned}
&\varepsilon^4 \, \frac{w^{n+1}(\xi) - 2\phi_1(\alpha) w^n(\xi) + w^{n-1}(\xi)}{\tau^2 \, \psi_1(\alpha)} \\
&- 2\varepsilon^3 c_g \, \frac{(w^{n+1}(\xi+h) - w^{n-1}(\xi+h)) - (w^{n+1}(\xi-h) - w^{n-1}(\xi-h))}{4\mathrm{sinc}(\alpha)\mathrm{sinc}(\beta)\tau h} \\
&+ \varepsilon^2 (c_g^2 - 1) \, \frac{w^n(\xi+h) - 2\phi_2(\beta) w^n(\xi) + w^n(\xi-h)}{h^2 \, \psi_2(\beta)} + v^n(\xi) = 0
\end{aligned} \tag{5.1}$$

We clearly have $w^n(\xi_j) = w_j^n$ of (3.2) for all $n \geqslant 2$ if this holds true for $n = 0$ and $n = 1$. In particular, we have $\max_j |w_j^n| \leqslant \max_{\xi\in\mathbb{T}} |w^n(\xi)| \leqslant \|w^n\|_{A(\mathbb{T})}$.

Lemma 5.1 (Linear stability of the filtered finite difference method) *Under condition* (3.5)*, the filtered finite difference algorithm* (5.1) *without the nonlinear term is stable: There exists a norm* $|||\cdot|||$ *on* $A(\mathbb{T})\times A(\mathbb{T})$*, equivalent to the norm* $\|\cdot\|_{A(\mathbb{T})\times A(\mathbb{T})}$ *uniformly in* ε,τ,h *subject to* (3.5)*, such that*

$$|||W^n||| = |||W^{n-1}|||, \qquad \text{where } W^n = \begin{pmatrix} w^{n+1} \\ w^n \end{pmatrix}.$$

Proof Let $\hat{w}^n = (\hat{w}_k^n)$ be the sequence of Fourier coefficients of v^n, i.e.,

$$w^n(\xi) = \sum_{k=-\infty}^{\infty} \mathrm{e}^{\mathrm{i}k\xi}\, \hat{w}_k^n.$$

Substituting this into (5.1) yields, for all j,

$$\sum_k \mathrm{e}^{\mathrm{i}kx_j}\Big(\varepsilon^4 \frac{\hat{w}_k^{n+1} - 2\phi_1(\alpha)\hat{w}_k^n + \hat{w}_k^{n-1}}{\tau^2\psi_1(\alpha)} - 2\varepsilon^3 c_g \frac{2\mathrm{i}\sin(kh)(\hat{w}_k^{n+1} - \hat{w}_k^{n-1})}{4\mathrm{sinc}(\alpha)\mathrm{sinc}(\beta)\tau h} + \varepsilon^2(c_g^2-1)\frac{2(\cos(kh)-\phi_2(\beta))\hat{w}_k^n}{h^2\psi_2(\beta)} + \hat{w}_k^n\Big) = 0,$$

and thus

$$\varepsilon^4 \frac{\hat{v}_k^{n+1} - 2\phi_1(\alpha)\hat{v}_k^n + \hat{v}_k^{n-1}}{\tau^2\psi_1(\alpha)} - \frac{\mathrm{i}\varepsilon^3 c_g \sin(kh)(\hat{v}_k^{n+1} - \hat{v}_k^{n-1})}{\mathrm{sinc}(\alpha)\mathrm{sinc}(\beta)\tau h} + \varepsilon^2(c_g^2-1)\frac{2(\cos(kh)-\phi_2(\beta))\hat{v}_k^n}{h^2\psi_2(\beta)} + \hat{v}_k^n = 0,$$

which is equivalent to the system

$$\begin{pmatrix} \hat{w}_k^{n+1} \\ \hat{w}_k^n \end{pmatrix} = G_k \begin{pmatrix} \hat{w}_k^n \\ \hat{w}_k^{n-1} \end{pmatrix},$$

where

$$G_k = \begin{pmatrix} \frac{2\phi_1(\alpha)-c_2}{1-\mathrm{i}c_1} & -\frac{1+\mathrm{i}c_1}{1-\mathrm{i}c_1} \\ 1 & 0 \end{pmatrix} \tag{5.2}$$

with

$$c_1 = \frac{c_g\tau\sin(kh)\psi_1(\alpha)}{\varepsilon h\mathrm{sinc}(\alpha)\mathrm{sinc}(\beta)}$$
$$c_2 = \frac{2\tau^2(c_g^2-1)(\cos(kh)-\phi_2(\beta))\psi_1(\alpha)}{\varepsilon^2h^2\psi_2(\beta)} + \frac{\tau^2\psi_1(\alpha)}{\varepsilon^4}.$$

Let λ_k^+, λ_k^- be the two roots of the characteristic polynomial

$$\rho_k(\zeta) = (1-\mathrm{i}c_1)\zeta^2 - (2\phi_1(\alpha)-c_2)\zeta + (1+\mathrm{i}c_1),$$

i.e.,

$$\lambda_k^{\pm} = \frac{2\phi_1(\alpha) - c_2 \pm \sqrt{(2\phi_1(\alpha)-c_2)^2 - 4(1+c_1^2)}}{2(1-\mathrm{i}c_1)}.$$

Under condition (3.5), we have

$$|2\phi_1(\alpha) - c_2| \leqslant 2|\phi_1(\alpha)| + |c_2| \leqslant 2r < 2\sqrt{1+c_1^2},$$

and thus $|\lambda_k^{\pm}| = 1$. The vectors $(\lambda_k^+, 1)^\top$ and $(\lambda_k^-, 1)^\top$ are eigenvectors of G_k with eigenvalue λ_k^+ and λ_k^-, respectively. This is because (similar for λ_k^-)

$$\begin{pmatrix} \frac{2\phi_1(\alpha)-c_2}{1-\mathrm{i}c_1} & -\frac{1+\mathrm{i}c_1}{1-\mathrm{i}c_1} \\ 1 & 0 \end{pmatrix} \begin{pmatrix} \lambda_k^+ \\ 1 \end{pmatrix} = \begin{pmatrix} \frac{(2\phi_1(\alpha)-c_2)\lambda_k^+ - (1+\mathrm{i}c_1)}{1-\mathrm{i}c_1} \\ \lambda_k^+ \end{pmatrix} = \lambda_k^+ \begin{pmatrix} \lambda_k^+ \\ 1 \end{pmatrix}.$$

Therefore G_k is diagonalizable,

$$P_k^{-1} G_k P_k = \Lambda_k = \mathrm{diag}\{\lambda_k^+, \lambda_k^-\}, \tag{5.3}$$

and Λ_k is a unitary matrix. Using the transformation matrix P_k, we have, for any vector $y \in \mathbb{C}^2$,

$$|P_k^{-1} G_k y|_2 = |\Lambda_k P_k^{-1} y|_2 = |P_k^{-1} y|_2.$$

Therefore,

$$\begin{aligned} |\!|\!| W^n |\!|\!| &:= \sum_k \left| P_k^{-1} \begin{pmatrix} \hat{w}_k^{n+1} \\ \hat{w}_k^n \end{pmatrix} \right|_2 = \sum_k \left| P_k^{-1} G_k \begin{pmatrix} \hat{w}_k^n \\ \hat{w}_k^{n-1} \end{pmatrix} \right|_2 \\ &= \sum_k \left| P_k^{-1} \begin{pmatrix} \hat{w}_k^n \\ \hat{w}_k^{n-1} \end{pmatrix} \right|_2 = |\!|\!| W^{n-1} |\!|\!|. \end{aligned}$$

Finally, we show that

$$\|P\|_2 := \max_k \|P_k\|_2 \leqslant C_1, \quad \|P^{-1}\|_2 := \max_k \|P_k^{-1}\|_2 \leqslant C_2,$$

which yields that the newly introduced norm $|\!|\!|\cdot|\!|\!|$ is equivalent to $\|\cdot\|_{A(\mathbb{T})\times A(\mathbb{T})}$. Since

$$P_k^* P_k = \begin{pmatrix} 2 & 1 + \overline{\lambda_k^+}\lambda_k^- \\ 1 + \overline{\lambda_k^-}\lambda_k^+ & 2 \end{pmatrix},$$

the eigenvalues of $P_k^* P_k$ can be calculated as $2\left(1 \pm \sqrt{\frac{(2\phi_1(\alpha)-c_2)^2}{4(1+c_1^2)}}\right)$. Since $\frac{(2\phi_1(\alpha)-c_2)^2}{4(1+c_1^2)} \leqslant r^2 < 1$ by condition (3.5), we have for all k that

$$\begin{aligned} \|P_k\|_2 &= \sqrt{\lambda_{\max}(P_k^* P_k)} < 2, \\ \|P_k^{-1}\|_2 &= 1/\sqrt{\lambda_{\min}(P_k^* P_k)} \leqslant 1/\sqrt{2(1-r)}, \end{aligned}$$

so that

$$\tfrac{1}{2}\|W\|_{A(\mathbb{T})\times A(\mathbb{T})} \leqslant |\!|\!| W |\!|\!| \leqslant \frac{1}{\sqrt{2(1-r)}} \|W\|_{A(\mathbb{T})\times A(\mathbb{T})}$$

for all $W \in A(\mathbb{T}) \times A(\mathbb{T})$. □

5.2 Nonlinear stability

Lemma 5.2 (Nonlinear stability of the filtered finite difference method) *Let the function $w^+ \in C([0,T], A(\mathbb{T}))$ be arbitrary and let the corresponding defect d be defined by (4.2). Under condition (3.5), the interpolated numerical solution of (3.2), interpolated to all $\xi \in \mathbb{T}$ as in (5.1) (but now with the nonlinear term included), satisfies the bound, for $t_n = n\tau \leqslant T$*

$$\begin{aligned}&\|w^{+,n} - A^+(t_n,\cdot)\|_{A(\mathbb{T})}\\ &\qquad \leqslant C\Big(\|w^{+,0} - A^+(0,\cdot)\|_{A(\mathbb{T})} + \|w^{+,1} - A^+(t_1,\cdot)\|_{A(\mathbb{T})} + \|d\|_{C([0,T],A(\mathbb{T}))}\Big),\end{aligned}$$

where C is independent of ε, τ, h, and n with $t_n \leqslant T$, but depends on T and on upper bounds of the above term in big brackets and of the $C([0,T],A(\mathbb{T}))$ norm of A^+.

Proof We define the error function $e^n(\xi) = w^{+,n}(\xi) - A^+(t_n,\xi)$, which satisfies

$$\begin{aligned}e^{n+1}(\xi) + e^{n-1}(\xi) &= \frac{\tau^2\psi_1(\alpha)(1-c_g^2)}{\varepsilon^2h^2\psi_2(\beta)}\big(e^n(\xi+h) - 2\phi(\beta)e^n(\xi) + e^n(\xi-h)\big)\\ &+ \frac{c_g\tau\psi_1(\alpha)}{2\varepsilon h\mathrm{sinc}(\alpha)\mathrm{sinc}(\beta)}\big((e^{n+1}(\xi+h) - e^{n-1}(\xi+h)) - (e^{n+1}(\xi-h) - e^{n-1}(\xi-h))\big)\\ &+ \left(2\phi_1(\alpha) - \frac{\tau^2\psi_1(\alpha)}{\varepsilon^4}\right)e^n(\xi) - \frac{\tau^2\psi_1(\alpha)}{\varepsilon^4}d(t_n,\xi)\\ &- \frac{\lambda\tau^2\psi_1(\alpha)}{\varepsilon^2\mathrm{tanc}^2(\beta)}\left(|w^{+,n}(\xi)|^2w^{+,n}(\xi) - |A^+(t_n,\xi)|^2A^+(t_n,\xi)\right).\end{aligned} \tag{5.4}$$

The Fourier coefficient of e^n then satisfies

$$\begin{aligned}\hat e_k^{n+1} + \hat e_k^{n-1} &= \left(\frac{2\tau^2\psi_1(\alpha)(1-c_g^2)(\cos(kh) - \phi_2(\beta))}{\varepsilon^2h^2\psi_2(\beta)} + \left(2\phi_1(\alpha) - \frac{\tau^2\psi_1(\alpha)}{\varepsilon^4}\right)\right)\hat e_k^n\\ &+ \frac{\mathrm{i}c_g\tau\psi_1(\alpha)\sin(kh)}{\varepsilon h\mathrm{sinc}(\alpha)\mathrm{sinc}(\beta)}(\hat e_k^{n+1} - \hat e_k^{n-1})\\ &+ \lambda\tau\sin(\alpha)\omega^{-1}\mathcal{F}\left(|w^{+,n}(\xi)|^2w^{+,n}(\xi) - |A^+(t_n,\xi)|^2A^+(t_n,\xi)\right)\\ &+ \tau\sin(\alpha)\omega^{-1}\rho^{-1}\hat d_k^n\end{aligned}$$

where we used (3.4) in the last term. This equation is equivalent to the one-step formulation

$$\begin{aligned}\begin{pmatrix}\hat e_k^{n+1}\\ \hat e_k^n\end{pmatrix} = G_k\begin{pmatrix}\hat e_k^n\\ \hat e_k^{n-1}\end{pmatrix} &+ \lambda\tau\sin(\alpha)\omega^{-1}\begin{pmatrix}\mathcal{F}\left(|u^n|^2u^n - |v^n|^2v^n\right)(k)\\ 0\end{pmatrix}\\ &+ \tau\sin(\alpha)\omega^{-1}\rho^{-1}\begin{pmatrix}\hat d_k^n\\ 0\end{pmatrix},\end{aligned}$$

where G_k is defined in (5.2).

Introducing $\mathcal{E}^n = \begin{pmatrix} e^{n+1} \\ e^n \end{pmatrix}$, using Lemma 5.1 and (4.7) for dealing with the nonlinearity, we obtain

$$\begin{aligned}
|||\mathcal{E}^n||| &\leqslant (1+c\tau)|||\mathcal{E}^{n-1}||| + \widetilde{c}\tau\|d(t_n,\cdot)\|_{A(\mathbb{T})} \\
&\leqslant (1+c\tau)^n|||\mathcal{E}^0||| + \widetilde{c}\tau\sum_{j=1}^{n}(1+c\tau)^{n-j}\|d(t_j,\cdot)\|_{A(\mathbb{T})} \\
&\leqslant \exp(cn\tau)|||\mathcal{E}^0||| + \widetilde{c}\tau\frac{\exp(cn\tau)-1}{c\tau}\sup_{t\in[0,T]}\|d(t,\cdot)\|_{A(\mathbb{T})},
\end{aligned}$$

which yields the result. □

Combined with Lemma 4.2 (consistency), Lemma 5.2 (stability) proves Theorem 3.1 with the $O(\tau^2+h^2+\varepsilon)$ remainder bound in the Wiener algebra norm, which is stronger than the maximum norm and hence this yields the same bound in the maximum norm. For the velocity approximation (3.3) , using (4.3) gives

$$\varepsilon^2 v_j^{+,n} = -\mathrm{i}\omega A^+(t^n,\xi_j) + O(\tau^2+h^2+\varepsilon^2).$$

Theorem 3.1 together with Proposition 2.1 further implies the error bounds of Theorem 3.2.

6 Numerical experiments

In this section, we consider the following 1-dimensional Klein–Gordon equation

$$\varepsilon^2\partial_{tt}u - \partial_{xx}u + \frac{1}{\varepsilon^2}u + \lambda|u|^2u = 0, \quad x\in\mathbb{R}$$

with $\lambda = 1$ and the initial value

$$u(0,x) = \mathrm{e}^{-x^2}\mathrm{e}^{\mathrm{i}x/\varepsilon}, \quad \partial_t u(0,x) = \frac{\mathrm{i}}{\varepsilon^2}\mathrm{e}^{-x^2}\mathrm{e}^{\mathrm{i}x/\varepsilon}.$$

As discussed in Remark 3.2, we first test our algorithm for large $\varepsilon = 1$. In this regime, our method converges to the standard leapfrog scheme, exhibiting second-order accuracy, as shown in the first plot in Figure 6.1. The errors are measured at the final time $t = 1$ using the discrete L^∞ norm over the spatial domain $[-4,4]$. The reference solution is computed by solving the original equation (1.1) with Fourier collocation with 6000 grid points in space and Strang splitting with a time step $5\varepsilon\cdot 10^{-4}$ in time.

While the method behaves like the standard leapfrog scheme for large ε, its performance in the small ε regime is more crucial for applications.

To satisfy the consistency condition (3.4) we first set ρ and then obtain β by solving the nonlinear equation $\varepsilon^2/\tan^2(\beta) = \rho$, which can be accomplished using the "fsolve" function in MATLAB. The size of the mesh h can be determined immediately after obtaining β. Similarly, we can find α by

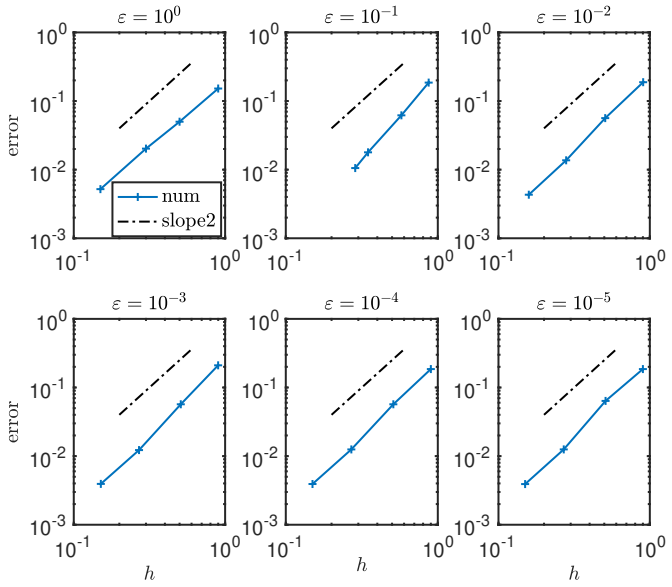

Fig. 6.1 Error vs. h with different ε for filtered finite difference method.

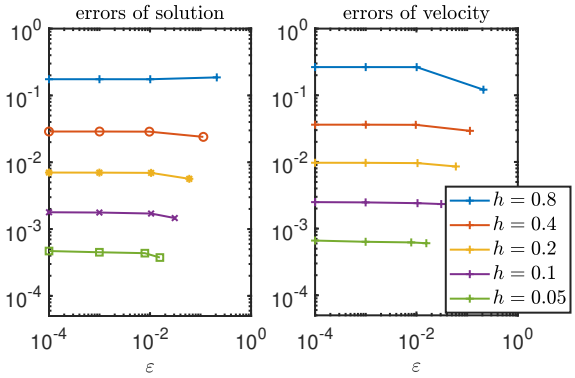

Fig. 6.2 Error vs. ε with different h for filtered finite difference method.

solving the relation $\varepsilon^2 \operatorname{sinc}(\alpha)/\psi_1(\alpha) = -\omega\rho/(\kappa c_g - \omega)$ with the initial guess $\alpha = (\kappa c_g - \omega)h^2/\varepsilon^2$. In this example, we set $\rho = 1$.

To test the order of our method for small ε $(10^{-1}, 10^{-2}, 10^{-3}, 10^{-4}, 10^{-5})$, we evaluate the error $(w_j^{+,n} - A^+(t^n, \xi_j))$, since Theorem 3.2 follows directly from Theorem 3.1. The error is measured at the final time $t = 1$ using the discrete counterpart of the maximum norm on $[-4, 4]$. The reference solution is obtained by solving the first Schrödinger equation (2.2) using Fourier collocation with 6000 grid points in space and Strang splitting with a time step 10^{-4} in time. As shown in Figure 6.1, second-order accuracy is observed for small ε with relatively large mesh sizes which is consistent with Theorem 3.1.

Figure 6.2 presents the errors in both the solution $(w_j^{+,n} - A^+(t^n, \xi_j))$ and the velocity $\varepsilon^2(v_j^{+,n} + \mathrm{i}\omega A^+(t^n, \xi_j))$ at time $t = 1$ versus ε for various mesh sizes h. The errors tend to a constant error level proportional to h^2, as expected.

Acknowledgement

This work was supported by the Deutsche Forschungsgemeinschaft (DFG, German Research Foundation) – Project-ID258734477 – SFB 1173.

References

1. W. Bao, Y. Cai, and X. Zhao. A uniformly accurate multiscale time integrator pseudospectral method for the Klein–Gordon equation in the nonrelativistic limit regime. *SIAM Journal on Numerical Analysis*, 52(5):2488–2511, 2014.
2. W. Bao and X. Dong. Analysis and comparison of numerical methods for the Klein–Gordon equation in the nonrelativistic limit regime. *Numerische Mathematik*, 120(2):189–229, 2012.
3. W. Bao and X. Zhao. Comparison of numerical methods for the nonlinear Klein–Gordon equation in the nonrelativistic limit regime. *Journal of Computational Physics*, 398:108886, 2019.
4. J. Baumstark, T. Jahnke, and C. Lubich. Polarized high-frequency wave propagation beyond the nonlinear Schrödinger approximation. *SIAM Journal on Mathematical Analysis*, 56(1):454–473, 2024.
5. S. Baumstark, E. Faou, and K. Schratz. Uniformly accurate exponential-type integrators for Klein–Gordon equations with asymptotic convergence to the classical NLS splitting. *Mathematics of Computation*, 87(311):1227–1254, 2018.
6. P. Chartier, N. Crouseilles, M. Lemou, and F. Méhats. Uniformly accurate numerical schemes for highly oscillatory Klein–Gordon and nonlinear Schrödinger equations. *Numerische Mathematik*, 129:211–250, 2015.
7. N. Crouseilles, S. Jin, and M. Lemou. Nonlinear geometric optics method-based multiscale numerical schemes for a class of highly oscillatory transport equations. *Mathematical Models and Methods in Applied Sciences*, 27(11):2031–2070, 2017.
8. X. Dong, Z. Xu, and X. Zhao. On time-splitting pseudospectral discretization for nonlinear Klein–Gordon equation in nonrelativistic limit regime. *Communications in Computational Physics*, 16(2):440–466, 2014.
9. E. Faou and K. Schratz. Asymptotic preserving schemes for the Klein–Gordon equation in the non-relativistic limit regime. *Numerische Mathematik*, 126(3):441–469, 2014.
10. W. Gautschi. Numerical integration of ordinary differential equations based on trigonometric polynomials. *Numerische Mathematik*, 3:381–397, 1961.
11. T. Jahnke and J. Mödl. Analytical and numerical approximations to highly oscillatory solutions of nonlinear Friedrichs systems. *CRC 1173 Preprint 2024/22, KIT*, 2024.
12. Y. Katznelson. *An introduction to harmonic analysis*. Dover Publications, Inc., New York, corrected edition, 1976.
13. P. Kirrmann, G. Schneider, and A. Mielke. The validity of modulation equations for extended systems with cubic nonlinearities. *Proceedings of the Royal Society of Edinburgh: Section A Mathematics*, 122(1–2):85–91, 1992.
14. R. D. Pierce and C. E. Wayne. On the validity of mean-field amplitude equations for counterpropagating wavetrains. *Nonlinearity*, 8(5):769, 1995.
15. Y. Shi and C. Lubich. Filtered finite difference methods for nonlinear Schrödinger equations in semiclassical scaling. *arXiv preprint arXiv:2411.07855*, 2024.